

# Multiple Phosphorylations in the C-terminal Tail of Plant Plasma Membrane Aquaporins

ROLE IN SUBCELLULAR TRAFFICKING OF *AtPIP2;1* IN RESPONSE TO SALT STRESS<sup>\*S</sup>

Sodana Prak<sup>‡</sup>, Sonia Hem<sup>§¶</sup>, Julie Boudet<sup>‡</sup>, Gaëlle Viennois<sup>‡</sup>, Nicolas Sommerer<sup>§</sup>, Michel Rossignol<sup>§</sup>, Christophe Maurel<sup>‡</sup>, and Véronique Santoni<sup>‡||</sup>

Aquaporins form a family of water and solute channel proteins and are present in most living organisms. In plants, aquaporins play an important role in the regulation of root water transport in response to abiotic stresses. In this work, we investigated the role of phosphorylation of plasma membrane intrinsic protein (PIP) aquaporins in the *Arabidopsis thaliana* root by a combination of quantitative mass spectrometry and cellular biology approaches. A novel phosphoproteomics procedure that involves plasma membrane purification, phosphopeptide enrichment with TiO<sub>2</sub> columns, and systematic mass spectrometry sequencing revealed multiple and adjacent phosphorylation sites in the C-terminal tail of several *AtPIPs*. Six of these sites had not been described previously. The phosphorylation of *AtPIP2;1* at two C-terminal sites (Ser<sup>280</sup> and Ser<sup>283</sup>) was monitored by an absolute quantification method and shown to be altered in response to treatments of plants by salt (NaCl) and hydrogen peroxide. The two treatments are known to strongly decrease the water permeability of *Arabidopsis* roots. To investigate a putative role of Ser<sup>280</sup> and Ser<sup>283</sup> phosphorylation in aquaporin subcellular trafficking, *AtPIP2;1* forms mutated at either one of the two sites were fused to the green fluorescent protein and expressed in transgenic plants. Confocal microscopy analysis of these plants revealed that, in resting conditions, phosphorylation of Ser<sup>283</sup> is necessary to target *AtPIP2;1* to the plasma membrane. In addition, a NaCl treatment induced an intracellular accumulation of *AtPIP2;1* by exerting specific actions onto *AtPIP2;1* forms differing in their phosphorylation at Ser<sup>283</sup> to induce their accumulation in distinct intracellular structures. Thus, the present study documents stress-induced quantitative changes in aquaporin phosphorylation and establishes for the first time a link with plant aquaporin subcellular localization. *Molecular & Cellular Proteomics* 7:1019–1030, 2008.

Aquaporins form a family of channel proteins that mediate the transport across membranes of water, small neutral solutes, and occasionally ions (1–3). Aquaporins are present in all living kingdoms and in plants. Aquaporins exhibit a characteristically high multiplicity of forms with for instance 35 members in *Arabidopsis* (4, 5). Based upon their amino acid sequence homology, plant aquaporins can be classified into four subfamilies (4–6). One of these corresponds to the plasma membrane intrinsic proteins (PIPs).<sup>1</sup> The PIPs with 13 members in *Arabidopsis* represent the most abundant aquaporins in the plasma membrane (PM) and can be further divided into two sequence homology groups (*AtPIP1* and *AtPIP2*). Aquaporins are 25–35-kDa proteins that share a typical organization with six transmembrane  $\alpha$ -helices interrupted by five connecting loops (loops A–E) (7, 8). In PM aquaporins, the N and C termini as well as loops B and D are exposed in the cytosol, whereas loops A, C, and E face the cell wall.

Plants need to continuously adjust their water status in response to changing environmental conditions, and aquaporins play an important role in these processes (3, 9, 10). In particular, physiological and genetics studies have provided compelling evidence for a role of aquaporins in the regulation, in response to abiotic stresses, of root water transport, *i.e.* root hydraulic conductivity ( $L_p$ ) (10, 11). For instance, exposure of *Arabidopsis* plants to salt (100 mM NaCl) induced a rapid (half-time, 45 min) and significant decrease (–70%) in  $L_p$  that was maintained for at least 24 h (12). Whereas the long term effect of this NaCl stress can be accounted for by an overall transcriptional down-regulation of aquaporins, the molecular mechanisms involved in the early inhibition of  $L_p$  by NaCl are not fully understood yet. These mechanisms involve a slight decrease in overall abundance of *AtPIP1* proteins as soon as 30 min after exposure to NaCl and a trafficking of *AtPIP1* and *AtPIP2* isoforms between the PM and intracellular compartments that may contribute to reducing the abundance of *AtPIPs* at the PM and therefore the hydraulic conductivity of salt-stressed root cells (12). Chilling is another stress that leads to inhibition of  $L_p$ , and a relationship

From the <sup>‡</sup>Biochimie et Physiologie Moléculaire des Plantes, SupAgro/Institut National de la Recherche Agronomique (INRA)/CNRS/UMR 5004, 2 place Viala, F-34060 Montpellier cedex 1, France and <sup>§</sup>Laboratoire de Protéomique Fonctionnelle, INRA UR 1199, 2 place Viala, F-34060 Montpellier cedex 1, France

Received, November 29, 2007, and in revised form, January 25, 2008

Published, MCP Papers in Press, January 29, 2008, DOI 10.1074/mcp.M700566-MCP200

<sup>1</sup> The abbreviations used are: PIP, plasma membrane intrinsic protein; GFP, green fluorescent protein;  $L_p$ , root hydraulic conductivity; PM, plasma membrane; TiO<sub>2</sub>, titanium dioxide; WT, wild type; ER, endoplasmic reticulum.

between aquaporin regulation and reactive oxygen species was established in this context (13). In cucumber for instance, hydrogen peroxide ( $H_2O_2$ ) accumulated in response to chilling, and treatment of roots with exogenous  $H_2O_2$  inhibited  $L_p$ , to the same extent as chilling. In *Arabidopsis* a rapid decrease in  $L_p$  can also be observed in response to 2 mM  $H_2O_2$ .<sup>2</sup> Because of its amplitude (>70%) and rapidity (half-time,  $\approx 8$  min) this decrease is undoubtedly due to a down-regulation of root aquaporins.

Post-translational modifications are central for regulating protein structure and function and thereby for modulating and controlling protein catalytic activity, subcellular localization, stability, and interaction with other partners. Qualitative and quantitative information about post-translational modifications and in particular measurements of their dynamic changes are now critically needed to understand the complexity of cell regulations. Protein phosphorylation is one of the most important and best characterized post-translational modifications. Virtually all cellular processes are regulated in one or multiple ways by reversible phosphorylation, and the identification of the protein kinases and phosphatases, their substrates, and the specific sites of phosphorylation involved is crucial for the understanding of cell signaling. Besides classical methods relying on *in vivo* and *in vitro* labeling or immunodetection of phosphorylated proteins, MS is now widely used for studies on protein phosphorylation (14, 15). Different instrumentations such as ESI- and MALDI-MS systems are now amenable to phosphoprotein analysis (16), and sample preparation procedures have been optimized to enhance phosphopeptide recovery and detection by MS (17). In particular, immobilized metal affinity chromatography (18) or titanium dioxide ( $TiO_2$ ) microcolumns (19) have proved powerful for the selective enrichment of phosphorylated peptides.

Phosphorylated serine residues have been identified in the N-terminal and C-terminal tails of various plant aquaporins (20–25). In particular, two phosphorylation sites were identified in the C terminus of *Arabidopsis* AtPIP2;1 (26) and AtPIP2;6 (25) and spinach SoPIP2;1 (22) (Table I). AtPIP2;7 also shows double phosphorylation, but only one phosphosite was clearly identified (26) (see Table I). Also all plant AtPIPs show a conserved putative phosphorylation site in loop B (22, 23). Based on functional analyses in *Xenopus* oocytes, it was proposed that phosphorylation of SoPIP2;1 at this site and at Ser<sup>262</sup> (in the C terminus) was able to regulate its water transport activity (22). A molecular mechanism for phosphorylation-dependent gating of PIPs has recently been proposed from the atomic structures of SoPIP2;1 in its open and closed conformations (8). Mammalian aquaporins also carry multiple phosphorylation sites, and by contrast to plant aquaporins, phosphorylation of mammalian aquaporin-2 is not involved in gating but rather regulates the shuttling of the protein between the PM and intracellular compartments (27, 28).

<sup>2</sup> Y. Boursiac, J. Boudet, O. Postaire, D.-T. Luu, C. Tournaire-Roux, and C. Maurel, submitted manuscript.

The purpose of this work was to study the role of plant PM aquaporin phosphorylation in regulating the root water permeability in response to NaCl and  $H_2O_2$  treatments. For this, a systematic inventory of phosphorylation sites in the C terminus of AtPIP aquaporins was performed, and novel phosphoresidues were discovered. Because of the emerging role of stimulus-dependent trafficking of plant aquaporins between the PM and intracellular compartments (12, 29, 30), the role of aquaporin phosphorylation in this process was investigated. The results point to a specific phosphorylated site in the C terminus of AtPIP2;1 that regulates the trafficking of this aquaporin in control conditions and in response to an NaCl treatment.

#### EXPERIMENTAL PROCEDURES

**Reagents**—Endoproteinase Lys-C was purchased from Calbiochem. Synthetic PIP2 peptides (<sup>277</sup>SLGSFRSAANV<sup>297</sup>), either unmodified or singly phosphorylated at Ser<sup>280</sup>, were isotopically labeled on Arg<sup>281</sup> with <sup>13</sup>C and <sup>15</sup>N to induce a 10-Da mass increment (Sigma). The same PIP2 peptide but diphosphorylated was isotopically labeled on Ala<sup>284</sup> and Ala<sup>285</sup> with <sup>13</sup>C to induce a 6-Da mass increment (NeoMPS, Strasbourg, France).  $TiO_2$  beads were obtained by disassembling  $TiO_2$  guard columns purchased from GL Sciences Inc. (Tokyo, Japan). The 3M Empore<sup>TM</sup> C<sub>8</sub> disks were from 3M Bioanalytical Technologies (St. Paul, MN). GELoader tips were from Eppendorf (Hamburg, Germany). 2,5-Hydroxybenzoic acid and  $\alpha$ -cyano-4-hydroxycinnamic acid were from Sigma-Aldrich. All other chemicals and reagents were of the highest commercially available grade.

**Plant Materials and Treatments**—*Arabidopsis thaliana* ecotype Columbia (Col-0), plants were cultivated in hydroponic conditions as described previously (31). Briefly plants were cultivated in a growth chamber at 20 °C with an 8-h light (150 microeinstein  $m^{-2} s^{-1}$ )/16-h dark cycle at 70% relative humidity. Plants were mounted on 35 × 35 × 0.6-cm polystyrene rafts floating in a basin filled with 8 liters of nutrient medium (1.25 mM KNO<sub>3</sub>, 0.75 mM MgSO<sub>4</sub>, 1.5 mM Ca(NO<sub>3</sub>)<sub>2</sub>, 0.5 mM KH<sub>2</sub>PO<sub>4</sub>, 0.1 mM Na<sub>2</sub>SiO<sub>3</sub>, 50  $\mu$ M FeEDTA, 50  $\mu$ M H<sub>3</sub>BO<sub>3</sub>, 12  $\mu$ M MnSO<sub>4</sub>, 1  $\mu$ M ZnSO<sub>4</sub>, 0.7  $\mu$ M CuSO<sub>4</sub>, 0.24  $\mu$ M MoO<sub>4</sub>(Na<sub>2</sub>) and cultivated for up to 7 weeks. The effects of NaCl and  $H_2O_2$  were then studied by complementing the nutrient solution with 100 mM NaCl for 2 and 4 h or 2 mM  $H_2O_2$  for 15 min prior to root excision. Transgenic seedlings were cultivated for 8 days on half-strength Murashige and Skoog medium (32) without any antibiotic selection. The plantlets were then transferred for 2 or 4 h into a nutrient solution as described above complemented or not with 100 mM NaCl.

**Purification of PIPs**—A microsomal fraction was obtained from roots (31). Plasma membrane vesicles were purified by aqueous two-phase partitioning of the microsomal fraction in a mixture of polyethylene glycol 3350/dextran T-500, 6.4% (w/w) each in the presence of 5 mM KCl, as described previously (31). Protein concentration was measured using a modified Bradford procedure (31). The mean yield of PM extraction was 20  $\mu$ g of protein/g of fresh weight. Extrinsic membrane proteins were stripped with a urea and NaOH treatment according to a previously described procedure (31). The abundance of AtPIP2 isoforms in PM samples was evaluated by an ELISA using an antibody raised against the last 17 amino acids of the AtPIP2;1 sequence as described previously (33). The mean yield of AtPIP2 isoform was 5.3 pmol of PIP2/ $\mu$ g of PM proteins. Proteins were separated by SDS-PAGE on 12% acrylamide gels (31).

**Protein Digestion and Phosphopeptide Purification**—The migrating band at 28 kDa was excised from SDS-PAGE and prepared for proteolytic digestion as described previously (31). Gel pieces containing 350 pmol of AtPIP2 aquaporins were reswollen in the presence of

Lys-C at an enzyme:aquaporin ratio of 1:25 at 37 °C for 16 h. The supernatant of the digest was collected, and the remaining peptides were extracted in 0.1% TFA, 60% acetonitrile by sonication for 15 min. Supernatants were pooled, and the final volume was reduced to 10  $\mu$ l using a centrifuge evaporator. To build up a TiO<sub>2</sub> microcolumn, a small piece was stamped out of an Empore C<sub>8</sub> disk by using a 200- $\mu$ l pipette tip and placed at the constricted end of the GELoader tip, and TiO<sub>2</sub> beads in suspension in acetonitrile were packed (34). The protein digest was then diluted in a loading buffer containing 80% acetonitrile and 0.1% TFA and loaded on the column, and the column was washed with 30  $\mu$ l of loading buffer. Phosphopeptides were eluted with 3  $\mu$ l of NH<sub>4</sub>OH at pH 12. 0.8  $\mu$ l of eluted peptides was mixed with 0.8  $\mu$ l of 20 mg/ml 2,5-hydroxybenzoic acid dissolved in acetonitrile, water, and phosphoric acid (50:44:6, v/v/v) and spotted onto the MALDI target for crystallization. The quantification of At-PIP2;1 C-terminal phosphorylation was performed by adding the synthetic labeled peptides corresponding to the C terminus of At-PIP2;1 (unmodified:singly phosphorylated:diphosphorylated, 1:1:3) to the protein digest prior to loading onto the TiO<sub>2</sub> column. The abundance of the unmodified form was quantified from the flow-through of the TiO<sub>2</sub> column. The flow-through was desalted using ZipTip  $\mu$ C<sub>18</sub> columns (Millipore, Bedford, MA). The desalted sample (0.8  $\mu$ l) was mixed with 0.8  $\mu$ l of matrix solution ( $\alpha$ -cyano-4-hydroxycinnamic acid at half-saturation in 1:1 (v/v) H<sub>2</sub>O/acetonitrile, 0.1% TFA) and spotted onto the MALDI target.

**Mass Spectrometric Analysis**—MALDI-TOF MS and MS/MS analyses were performed, in positive reflector mode, using an UltraFlex II mass spectrometer (Bruker Daltonics, Bremen, Germany) equipped with a smartbeam™ laser. MS/MS spectra were obtained by PSD-LIFT™ without adding a collision gas. MS data were analyzed using the FlexAnalysis software (Bruker Daltonics). All MS and MS/MS spectra shown were externally calibrated and are raw data spectra, *i.e.* without recalibrating, smoothing, or base-line subtracting. MS and MS/MS spectra annotation was performed manually. *De novo* sequencing was performed and was facilitated by the knowledge of all aquaporin sequences. All peptides proposed as phosphorylated were first checked for the presence of the major fragment ion [MH - H<sub>3</sub>PO<sub>4</sub>]<sup>+</sup> = MH - 98 Da corresponding to the loss of the phosphate moiety. In addition, all MS/MS spectra were carefully checked manually for assignment of phosphorylation sites.

**Gene Constructs and Expression in Transgenic Plants**—Mutagenesis of AtPIP2;1 C-terminal phosphorylation sites was carried out by PCR on a cDNA of AtPIP2;1 fused by its N terminus to the green fluorescent protein (GFP) (GFP-PIP2;1). For this, we used a sense primer containing an XhoI restriction site: 5'-TTTCTCGAGATGGT-GAGCAAGGGCGAGG-3'. The antisense primer allows the introduction of an XbaI restriction site as well as the desired mutation. The mutagenic primers used to generate the following mutations (bold characters) were: S280A, 5'-TTC TAG ATT AGA CGT TGG CAG CAC TTC TGA **ATG CTC** C-3'; S283A, 5'-TTC TAG ATT AGA CGT TGG **CAG CAG CTC TG**-3'; and S283D, 5'-TTT CTA GAT TAG ACG TTG GCA GCA **TCT CTG AA**-3'. The fragments amplified by PCR were digested by XhoI and XbaI and cloned in a pBluescript vector. The presence of the mutations was checked by DNA sequencing (Genoscreen, Lille, France). The GFP-PIP2;1 sequences were placed under the control of a cauliflower mosaic virus 35S and *RbcS* terminator by cloning into the EcoRI and ClaI sites of a pGREEN vector (35). The constructs were then transferred into *Agrobacterium tumefaciens* strain GV3101 by electroporation with a selection for tetracycline, rifampicin, and kanamycin resistance. The bacterial strains were used for transformation of *Arabidopsis* Col-0 by the floral dip method (36). To select for transformed plants, seeds were surface-sterilized and germinated in a medium containing a half-strength Murashige and Skoog medium (32) complemented with 7 g/liter agar and 0.04 g/liter

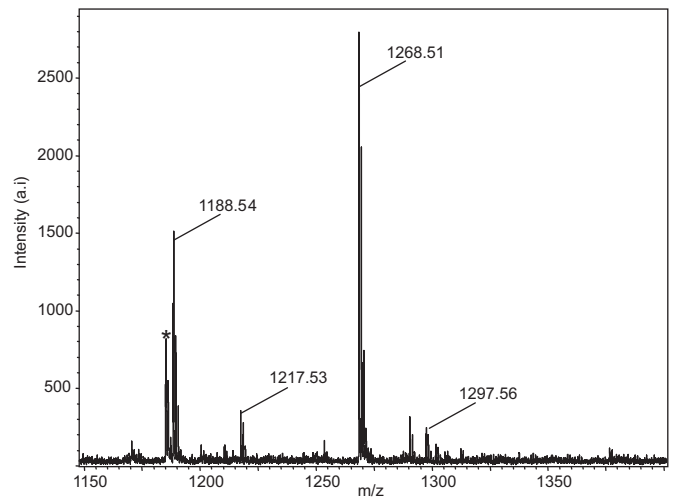


**FIG. 1. MALDI-TOF MS spectrum of phosphopeptides from plant PM aquaporins.** The 28-kDa band from root PM enriched in hydrophobic proteins was digested by Lys-C. Phosphopeptides were enriched using a TiO<sub>2</sub> column. All C-terminal phosphopeptides expected from root AtPIP aquaporins cannot be simultaneously recorded onto the same MS spectrum. The present spectrum illustrates the presence of the singly (*m/z* 1188.54) and diphosphorylated (*m/z* 1268.51) peptides of AtPIP2;1 and/or AtPIP2;2 (see text) and of the singly (*m/z* 1217.53) and diphosphorylated (*m/z* 1297.56) peptides of AtPIP2;7. \*, metastable decomposition of peptide with *m/z* 1268.51. *a.i.*, absolute intensity.

hygromycin as described previously (12). Two, three, two, and two independent lines were obtained for the GFP-PIP2;1, GFP-PIP2;1-S280A, GFP-PIP2;1-S283A, and GFP-PIP2;1-S283D genotypes, respectively.

**Microscopic Observations of Transgenic Plants**—The roots of transgenic lines expressing GFP-PIP2;1 fusions were observed under a confocal microscope (LSM 510 AX70, Zeiss, Göttingen, Germany) with two to three independent lines characterized for each construct. The argon laser wavelength was 488 nm; GFP emission was detected with the filter set for fluorescein isothiocyanate (bandwidth from 500 to 530 nm). The acquisition software used was LSM 510 version 3.0, and the image processing software was Zeiss LSM Image Browser. Cells were individually examined through a z series of images.

## RESULTS

**A Phosphoproteomics Analysis Reveals Novel Phosphorylation Sites in the C-terminal Tail of AtPIP Aquaporins**—A PM fraction was purified from *Arabidopsis* roots by aqueous two-phase partitioning and enriched in hydrophobic proteins with a urea and NaOH treatment (31). This extract was used to make a systematic inventory of the C-terminal phosphorylations of AtPIP2 isoforms. For this, the extract was first treated with the endoproteinase Lys-C, which is predicted to release the C-terminal tail of all AtPIP2 aquaporins. Phosphorylated C-terminal peptides were then enriched using TiO<sub>2</sub> microcolumns (19). A typical MALDI MS spectrum is shown in Fig. 1. The candidate phosphopeptides were initially assigned by MALDI-TOF MS from 79.96-Da mass increments per phosphate moiety relative to the unmodified peptides. During MALDI-TOF MS, phosphopeptides also lose phosphoric acid

TABLE I  
Phosphorylation sites in the C-terminal tail of PIP aquaporins

The first and second columns describe the name of the aquaporin and the peptide sequence, respectively. The third column (n\_ph) refers to the number of phosphorylation sites present in the peptide. pS, phosphorylated serine; pT, phosphorylated threonine.

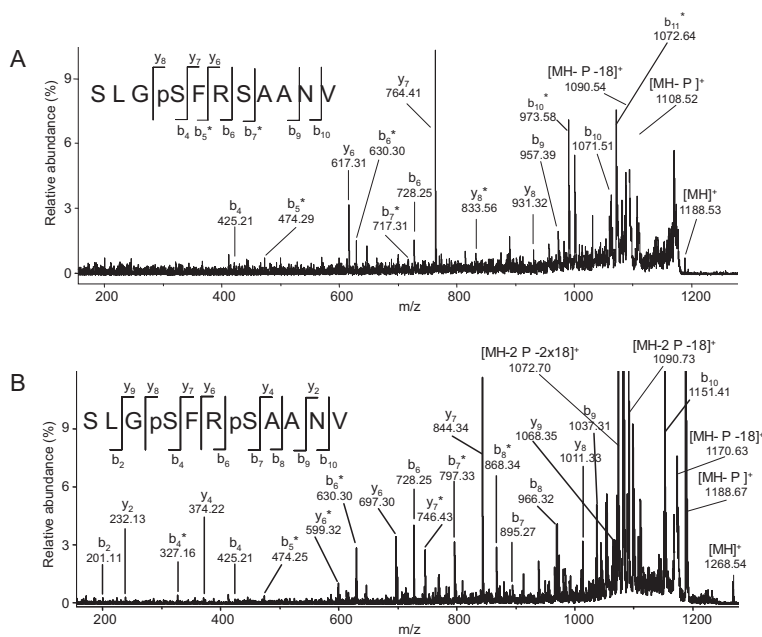
Protein	Sequence	n_ph	Ref.
AtPIP2;1/2;2/2;3	<sup>277</sup> SLGpSFR <sup>282</sup>	1	25, 31 <sup>a</sup>
AtPIP2;1/2;2/2;3	<sup>277</sup> SLGpSFRSAANV <sup>287</sup>	1	Present work
AtPIP2;1/2;2/2;3	<sup>277</sup> SLGpSFRpSAANV <sup>287</sup>	2	25, 26, and present work
AtPIP2;4	<sup>277</sup> ALGpSFGSFGSFRSFA <sup>291</sup>	1	Present work
AtPIP2;4	<sup>277</sup> ALGpSFGpSFGSFRSFA <sup>291</sup>	2	Present work
AtPIP2;4	<sup>277</sup> ALGpSFGpSFGpSFRsFA <sup>291</sup>	3	Present work
AtPIP2;4	<sup>277</sup> ALGpSFGpSFGSFRpSFA <sup>291</sup>	3	Present work
AtPIP2;6	<sup>282</sup> pSQLHELHA <sup>289</sup>	1	25
AtPIP2;7	<sup>270</sup> ALGpSFRSNATN <sup>280</sup>	1	Present work
AtPIP2;7	<sup>270</sup> ALGpSFRpSNATN <sup>280</sup>	2	26, 34, <sup>b</sup> and present work
AtPIP2;7	<sup>270</sup> ALGpSFRpSNApTN <sup>280</sup>	3	Present work
SoPIP2;1	<sup>271</sup> ALGpSFRSNPTN <sup>281</sup>	1	22
SoPIP2;1	<sup>271</sup> ALGpSFRpSNPTN <sup>281</sup>	2	22

<sup>a</sup> One phosphorylation site was detected but not identified.

<sup>b</sup> Two phosphorylation sites were detected, but only Ser<sup>273</sup> was identified as phosphorylated.

FIG. 2. Phosphopeptide sequencing by MALDI-TOF/TOF of the C-terminal tail of AtPIP2;1.

A, MS/MS spectrum of singly phosphorylated <sup>277</sup>SLGpSFRSAANV<sup>287</sup> (m/z 1188.53). y<sub>7</sub> and y<sub>8</sub> ions allowed identification of Ser<sup>280</sup> as the phosphorylated residue. B, MS/MS spectrum of the corresponding diphosphorylated peptide (m/z 1268.54). y<sub>4</sub>, y<sub>5</sub>, y<sub>7</sub>, and y<sub>9</sub> ions allowed identification of the two phosphorylated residues as Ser<sup>280</sup> and Ser<sup>283</sup>. \*, fragment ions arising from loss of phosphoric acid (-98 Da). pS, phosphorylated serine; [MH]<sup>+</sup>, precursor ion; [MH - P]<sup>+</sup>, precursor ion with a loss of one metaphosphoric acid (-80 Da); [MH - P - 18]<sup>+</sup>, precursor ion with a loss of one phosphoric acid (-98 Da); [MH - 2P - 18]<sup>+</sup>, precursor ion with a loss of one metaphosphoric acid (-80 Da) and one phosphoric acid (-98 Da); [MH - 2P - 2 × 18]<sup>+</sup>, precursor ion with a loss of two phosphoric acids (-196 Da).



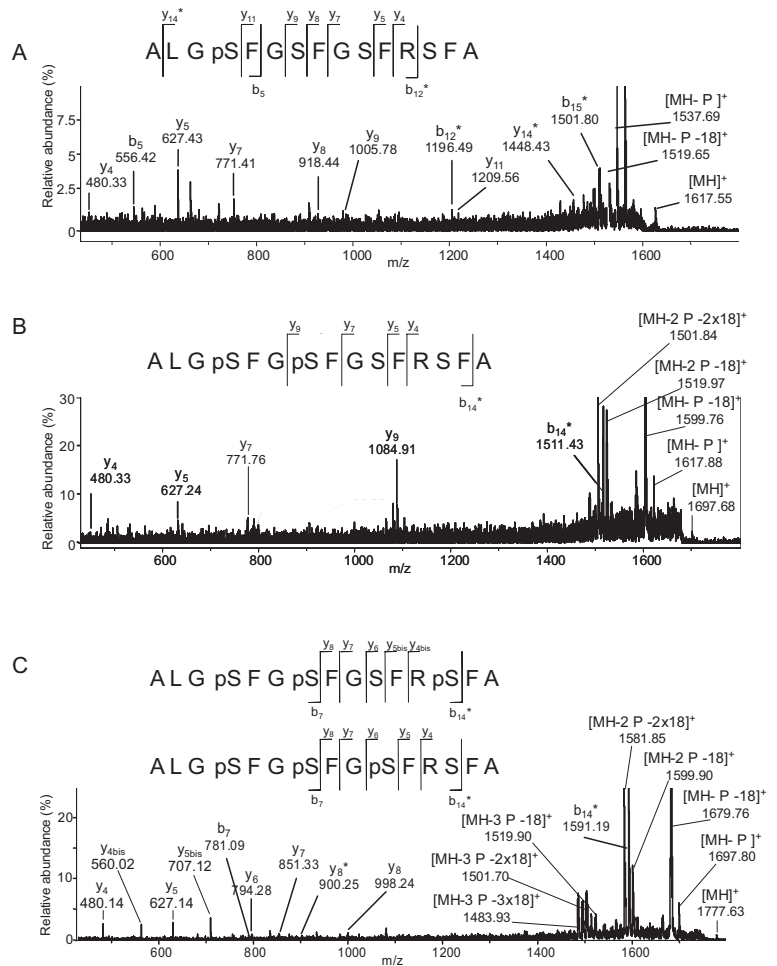
as H<sub>3</sub>PO<sub>4</sub> (98 Da) with the concomitant production of metastable ions with an apparent mass loss of 83 Da. Their presence was utilized as reliable indicators for phosphopeptides. A computational analysis of the mass spectra and comparison with the known aquaporin sequences allowed prediction of the presence of putative singly and diphosphorylated peptides of AtPIP2;1, AtPIP2;2, AtPIP2;3, AtPIP2;4, and AtPIP2;7 (Table I). In addition, triphosphorylated forms could be assigned to AtPIP2;4 and AtPIP2;7 isoforms (Table I). The putative phosphopeptides assigned to AtPIP isoforms were then sequenced by MALDI-TOF/TOF for confirmation and for identification of the phosphorylated residues. The positioning of the phosphorylated residue(s) was more specifically based on the

identification of dehydroalanine residue-containing ions in the MS/MS spectrum.

We note that AtPIP2;1 and AtPIP2;2 are among the most abundant aquaporins in roots (12, 31, 37). The phosphopeptides derived from these isoforms were systematically detected in MS spectra. By contrast, phosphopeptides attributed to the less abundant AtPIP2 isoforms such as AtPIP2;4 and AtPIP2;7 were only occasionally detected as shown in Fig. 1.

Because they share identical C-terminal sequences, the AtPIP2;1, AtPIP2;2, and AtPIP2;3 that were predicted to be singly and diphosphorylated could not be distinguished in our study. By contrast to AtPIP2;1 and AtPIP2;2, AtPIP2;3 is barely expressed in roots (31), and for the sake of simplifica-

**FIG. 3. Phosphopeptide sequencing by MALDI-TOF/TOF of the C-terminal tail of AtPIP2;4.** A, MS/MS spectrum of singly phosphorylated  $^{277}$ ALGSFGSFGSFRSFA $^{291}$  ( $m/z$  1617.55).  $b_5$  and  $y_{11}$  ions allowed identification of Ser $^{280}$  as the phosphorylated residue. B, MS/MS spectrum of the corresponding diphosphorylated peptide ( $m/z$  1697.68).  $y_4$ ,  $y_5$ ,  $y_7$ , and  $y_9$  ions allowed identification of phosphorylated Ser $^{280}$  and Ser $^{283}$ . C, MS/MS spectrum of the corresponding triphosphorylated peptide ( $m/z$  1777.63) that is a mixture of two forms:  $b_7$  ion allowed determination of the phosphorylation of the two residues Ser $^{280}$  and Ser $^{283}$ ,  $y_4$ ,  $y_5$ , and  $y_6$  ions indicated that Ser $^{286}$  can be phosphorylated;  $y_{4bis}$ ,  $y_{5bis}$ , and  $y_6$  showed that alternatively Ser $^{289}$  can carry the third phosphorylation. \*, pS, [MH] $^+$ , [MH - P] $^+$ , [MH - P - 18] $^+$ , [MH - 2P - 18] $^+$ , and [MH - 2P - 2 × 18] $^+$  are as explained in the legend of Fig. 2.



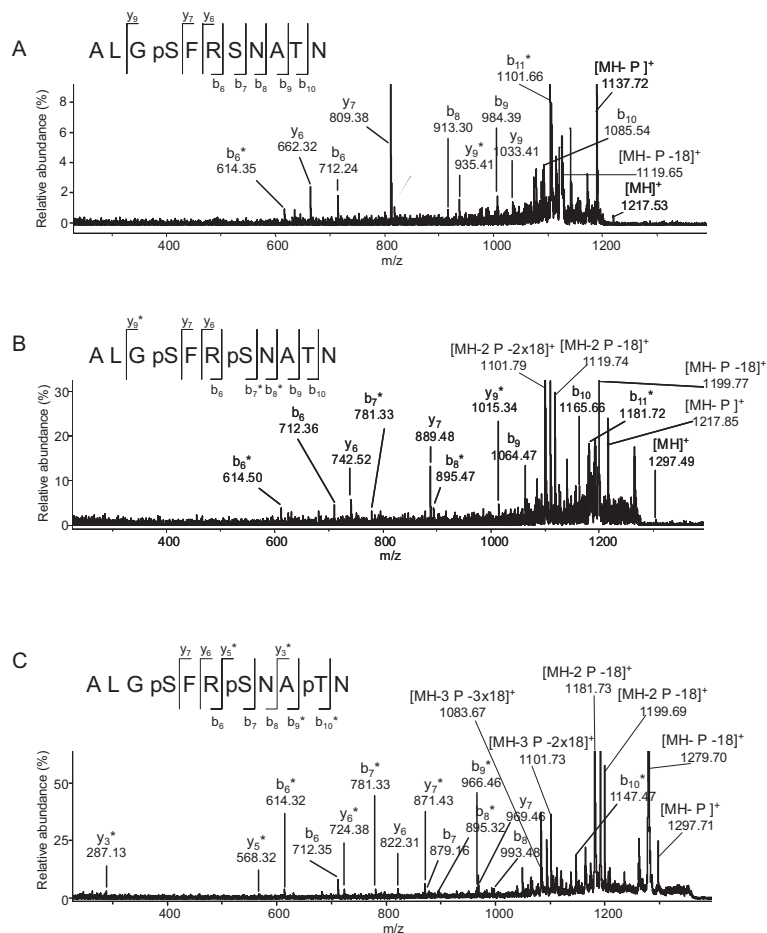
tion, these peptides were attributed to AtPIP2;1 here. Using this approach, the sequencing of the peptides at  $m/z$  1188.54 and  $m/z$  1268.51 revealed single and diphosphorylation of AtPIP2;1 on Ser $^{280}$  and Ser $^{280}$  and Ser $^{283}$ , respectively (Fig. 2). The fragmentation of the C-terminal peptides of AtPIP2;4 revealed a single phosphorylation on Ser $^{280}$  (peptide at  $m/z$  1617.55) and a diphosphorylation on Ser $^{280}$  and Ser $^{283}$  (peptide at  $m/z$  1697.68). The MS/MS analysis of a putative low abundance triphosphorylated peptide of AtPIP2;4 (peptide at  $m/z$  1777.63) revealed that it actually corresponded to a mixture of two isobaric forms of the AtPIP2;4 C-terminal tail (Fig. 3C). Sequencing showed a conserved phosphorylation at residues Ser $^{280}$  and Ser $^{283}$  and an additional phosphorylation of either Ser $^{286}$  or Ser $^{289}$ . The C-terminal tail of AtPIP2;7 was found to be singly phosphorylated on Ser $^{273}$  (peptide at  $m/z$  1217.53), diphosphorylated on Ser $^{273}$  and Ser $^{276}$  (peptide at  $m/z$  1297.49), or triphosphorylated on Thr $^{279}$  in addition to the two Ser residues (peptide at  $m/z$  1377.51) (Fig. 4). Table I summarizes all phosphorylation sites identified in this work. Table I shows that six new phosphorylation sites were identified in the C-terminal tail of aquaporins of *Arabidopsis* in addition to four previously known phosphorylation sites. This

work also allowed the discovery that not only Ser residues but also a Thr residue can be phosphorylated in plant aquaporins.

In theory, by considering all peptide forms, two, three, and four phosphorylation sites should result in peptides with four, eight, and 16 phosphorylation states, respectively. However, a lower number of peptides was observed in AtPIP2;1, AtPIP2;4, and AtPIP2;7, suggesting that phosphorylation events in these proteins might be interdependent. It appeared that phosphorylation of the most distal residues in a C-terminal sequence was only observed in association to phosphorylation of upstream neighboring Ser residue(s). In AtPIP2;1 for instance, Ser $^{283}$  was never found to be singly phosphorylated, and its phosphorylation was always associated to that of Ser $^{280}$ . Similarly in AtPIP2;7 phosphorylation of Thr $^{279}$  was linked to that of Ser $^{276}$ , which was itself linked to that of Ser $^{273}$ . In AtPIP2;4, the phosphorylation of the distal residues Ser $^{286}$  and Ser $^{289}$  appeared to be linked to phosphorylation of both Ser $^{280}$  and Ser $^{283}$ .

*C-terminal Phosphorylation of AtPIP2;1 Is Quantitatively Modified following Treatments of Plants with NaCl or H<sub>2</sub>O<sub>2</sub>*—AtPIP2;1 is one of most abundant aquaporins in *Arabidopsis* root and therefore must significantly contribute to L<sub>p</sub>, and to

**FIG. 4. Phosphopeptide sequencing by MALDI-TOF/TOF of the C-terminal tail of AtPIP2;7.** A, MS/MS spectrum of singly phosphorylated  $^{270}$ ALGSFRSNA-TN $^{280}$  ( $m/z$  1217.53).  $b_6$ ,  $y_7$ , and  $y_9$  ions allowed identification of the phosphorylated residue as Ser $^{273}$ . B, MS/MS spectrum of the corresponding diphosphorylated peptide ( $m/z$  1297.49).  $b_6$  and  $b_7$  ions allowed identification of Ser $^{273}$  and Ser $^{276}$  as the phosphorylated residues. C, MS/MS spectrum of the corresponding triphosphorylated peptide ( $m/z$  1377.51).  $b_6$ ,  $b_7$ ,  $b_{10}$ ,  $y_3$ , and  $y_5$  ions allowed identification of Ser $^{273}$ , Ser $^{276}$ , and Thr $^{279}$  as the phosphorylated residues. \*,  $pS$ ,  $[MH]^+$ ,  $[MH - P]^+$ ,  $[MH - P - 18]^+$ ,  $[MH - 2P - 18]^+$ , and  $[MH - 2P - 2 \times 18]^+$  are as explained in the legend of Fig. 2.  $pT$ , phosphorylated threonine.



its regulation. In addition, AtPIP2;1 displays a less complex phosphorylation pattern than other AtPIP2 isoforms. For these reasons, AtPIP2;1 was chosen as a model root aquaporin, and qualitative and/or quantitative changes in its C-terminal phosphorylation status in response to NaCl and H $_2$ O $_2$  treatments were investigated. MS/MS sequencing of the singly and diphosphorylated forms ( $m/z$  1188.53 and  $m/z$  1268.54) of AtPIP2;1 in plants exposed to a 2- or a 4-h treatment with 100 mM NaCl revealed that, as in control conditions, the singly phosphorylated residue was Ser $^{280}$  (supplemental Fig. 1) and that diphosphorylation had occurred on Ser $^{280}$  and Ser $^{283}$  (supplemental Fig. 2). Thus, the NaCl treatment did not qualitatively change the phosphorylation pattern of AtPIP2;1. Similar conclusions were obtained in plants treated by 2 mM H $_2$ O $_2$  for 15 min (data not shown).

The unmodified C-terminal AtPIP2;1 peptide and its singly and diphosphorylated forms were quantified using a strategy adapted from the absolute quantification method (38). For this, we used three reference synthetic peptides that, with respect to endogenous peptides, had incorporated stable isotopes. This labeling induced a mass increment of 10, 10, and 6 Da with respect to the unmodified, singly phosphorylated, and diphosphorylated endogenous peptides, respec-

tively (Fig. 5). The reference peptides were introduced into the peptide digest prior to the purification of phosphopeptides with TiO $_2$  microcolumns. The phosphorylated and unmodified peptides were quantified in the MALDI MS spectra arising from the elution of the microcolumns and from their flow-through, respectively. More specifically, native peptides were quantified from the ratio of the monoisotopic peak area of the native and of the corresponding reference peptide (Fig. 5). Four independent biological experiments were performed to quantitatively study the phosphorylation status of AtPIP2;1 in plants that had been exposed to a 2- or 4-h treatment with 100 mM NaCl or to a 15-min treatment with 2 mM H $_2$ O $_2$ . Fig. 6A shows that the 2- or 4-h NaCl treatment induced a statistically significant 30% decrease in the abundance of the diphosphorylated form (Mann and Whitney,  $p < 0.05$ ). A tendency toward an increase in abundance of the unmodified and singly phosphorylated forms was also observed in these experiments (Fig. 6A). By contrast, an H $_2$ O $_2$  treatment induced a statistically significant 2-fold decrease in abundance of the unmodified form (Mann and Whitney,  $p < 0.05$ ) (Fig. 6B). This decrease was accompanied by a slight relative (20%) increase in the abundance of the diphosphorylated form (Fig. 6B).

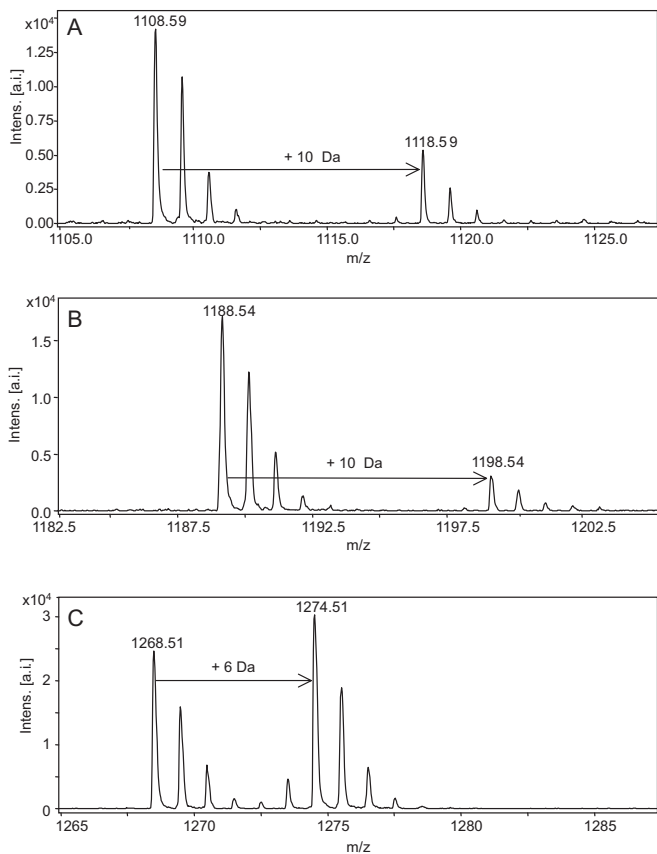


**FIG. 5. Principle for quantification of phosphorylation of the C-terminal tail of AtPIP2;1.** Synthetic peptides were added to the peptide digest prior to phosphopeptide enrichment on TiO<sub>2</sub> columns (see “Experimental Procedures”). The native and synthetic unmodified peptides (A) were purified from the column flow-through and analyzed by MS. Native and synthetic singly (B) and diphosphorylated (C) peptides were enriched after elution from the columns and analyzed by MS. The synthetic unmodified and singly phosphorylated peptides displayed a 10-Da mass increment when compared with their native counterparts (A and B). A 6-Da mass increment was displayed by the diphosphorylated synthetic peptide (C). The ratio between the monoisotopic peak surface of native and synthetic peptides was used to determine the absolute quantity of native peptides. The proportion of each C-terminal form of AtPIP2;1 in each sample was then calculated. Intens., intensity; a.i., absolute intensity.

*The Phosphorylation of Ser<sup>283</sup> Is Involved in the Targeting of AtPIP2;1 to the PM and in Its Intracellular Accumulation upon an NaCl Treatment*—The role of specific phosphorylated residues in gating plant aquaporins has been well described (8, 21, 22). By contrast, the role of phosphorylation in the regulation of plant aquaporin trafficking has not yet been investigated. We previously showed that a fusion of AtPIP2;1 with GFP labels the PM of root cells and that an NaCl treatment induces the additional labeling of intracellular structures, suggesting a relocation mechanism in response to NaCl (12).<sup>2</sup> The finding that an NaCl treatment decreased the phosphorylation of Ser<sup>283</sup> of AtPIP2;1 prompted us to investigate the role of this modification in the subcellular trafficking of the

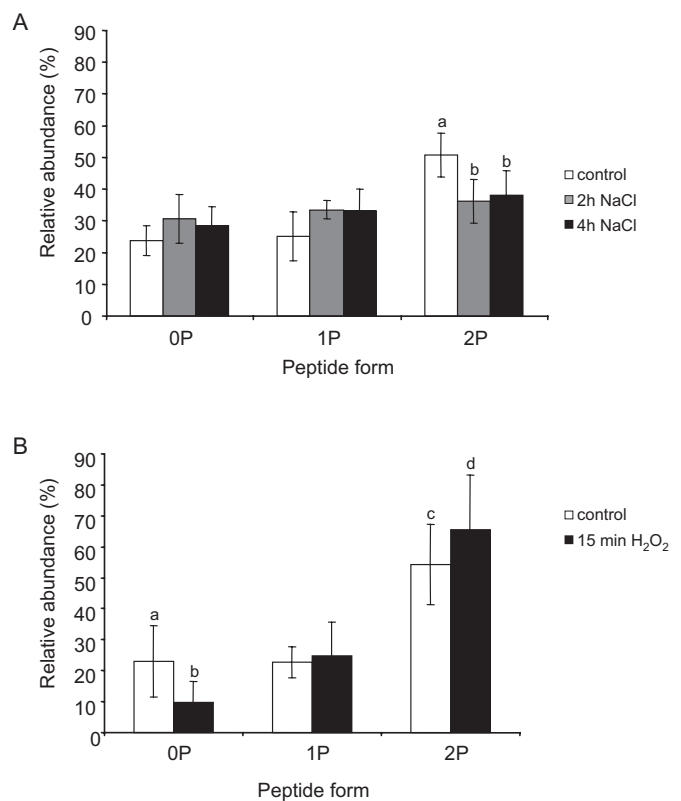


**FIG. 6. Quantification of C-terminal phosphorylation of AtPIP2;1 upon NaCl (A) and H<sub>2</sub>O<sub>2</sub> (B) treatments.** A, plants were either untreated (white bars) or treated with 100 mM NaCl for 2 h (gray bars) or 4 h (black bars). The proportion of the unmodified (0P), singly phosphorylated on Ser<sup>280</sup> (1P), and diphosphorylated on Ser<sup>280</sup> and Ser<sup>283</sup> (2P) peptides was quantified in plant extracts as exemplified in Fig. 5. Letters a–d indicate statistically different values (Mann and Whitney,  $p < 0.05$ ). B, plants were untreated (white) or treated with 2 mM H<sub>2</sub>O<sub>2</sub> for 15 min (black). The same procedures and conventions as in A were used.

protein. For this, GFP was fused to the N-terminal tail of AtPIP2;1, either wild type (WT) or carrying Ser to Ala mutations at positions 280 (S280A) or 283 (S283A) or a Ser to Asp mutation at position 283 (S283D). The fusion proteins were expressed in transgenic *Arabidopsis*, and their expression in epidermal cells at 1 cm from the apex was observed by laser-scanning confocal microscopy. In normal growth conditions, root cells of plants expressing the fusions of GFP with WT-PIP2;1 (GFP-PIP2;1) or the PIP2;1-S280A mutant (GFP-PIP2;1-S280A) showed a labeling pattern consistent with predominant localization of the proteins in the PM (Fig. 7A). By contrast, plants expressing GFP-PIP2;1-S283A showed an intracellular reticulation pattern in 40% of root cells (Fig. 7, A and B). Because of a pronounced localization around the nucleus and its fuzzy aspect throughout the cell, this intracellular staining was partly assigned to endoplasmic reticulum (ER) structures (39). Interestingly plants expressing GFP-PIP2;1-S283D, whereby the introduced mutation is supposed to mimic a constitutive phosphorylation at position 283, displayed a consistent PM staining in root cells

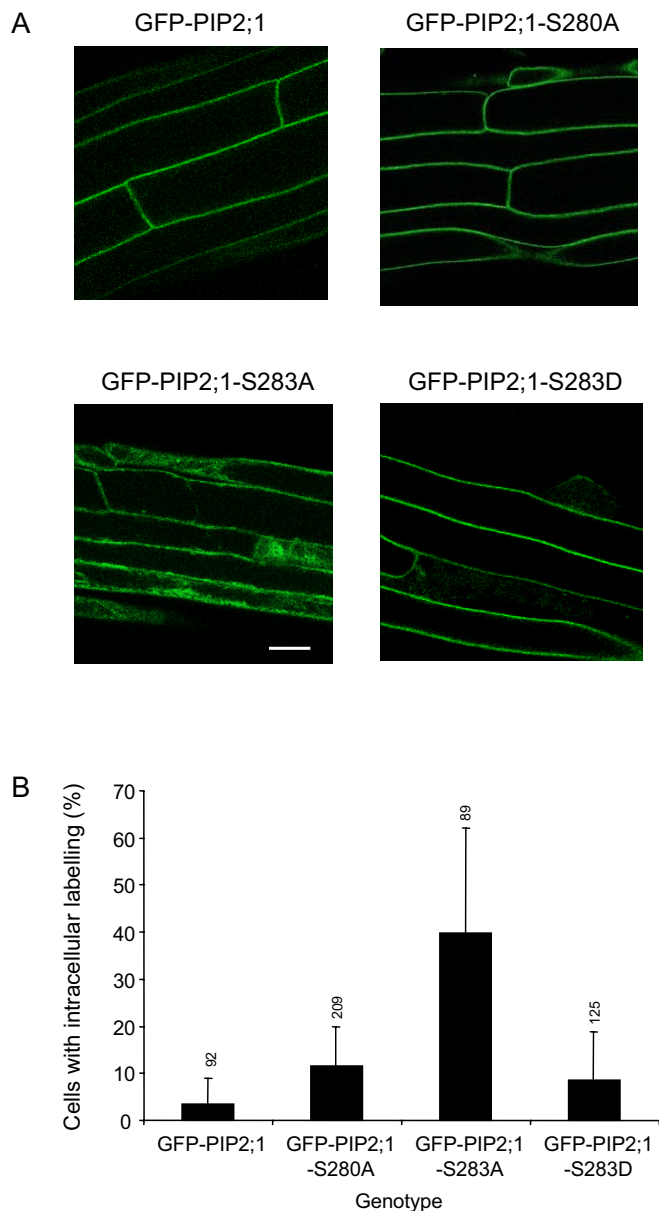


**FIG. 7. Role of C-terminal phosphorylation in the subcellular localization of AtPIP2;1.** *A*, the figure shows typical laser-scanning confocal micrographs of the fluorescence emitted by root epidermal cells at 1 cm from the apex in transgenic plants that express GFP-PIP2;1, GFP-PIP2;1-S280A, GFP-PIP2;1-S283A, or GFP-PIP2;1-S283D. Scale bar, 20  $\mu$ m. *B*, the graph represents the proportion of root cells at 1 cm from the apex with an intracellular staining. Data were obtained from transgenic plants that express the following constructs: GFP-PIP2;1 ( $n = 13$  plants from two independent transgenic lines), GFP-PIP2;1-S280A ( $n = 9$  plants from three independent transgenic lines), GFP-PIP2;1-S283A ( $n = 7$  plants from two independent transgenic lines), and GFP-PIP2;1-S283D ( $n = 6$  plants from two independent transgenic lines). The numbers on the graph correspond to the total number of observed cells. The error bars represent S.D.

(Fig. 7, *A* and *B*). Altogether these observations indicated that residue Ser<sup>283</sup>, and very likely its phosphorylation, is necessary for a proper targeting of AtPIP2;1 to the PM.

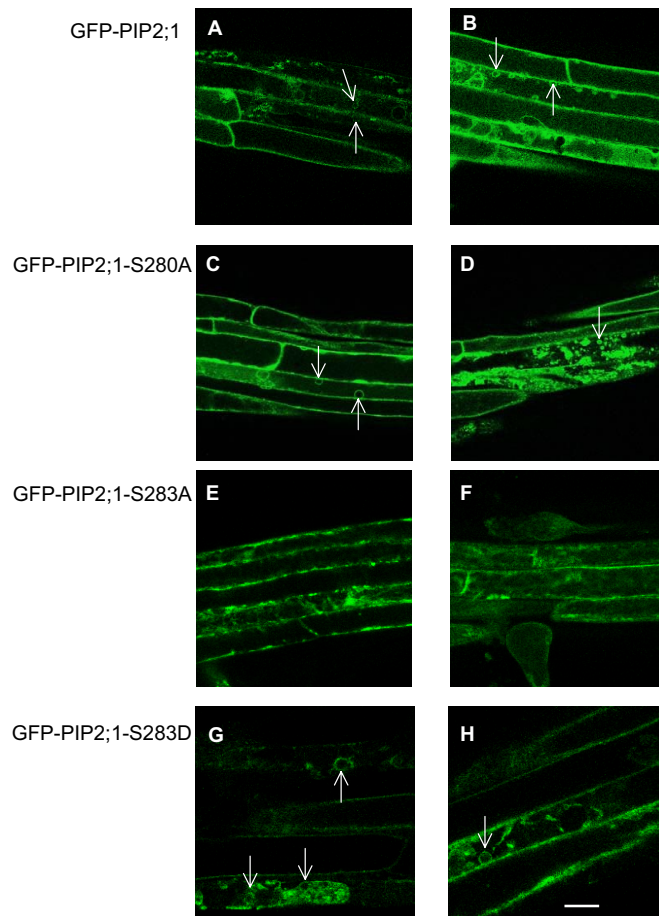
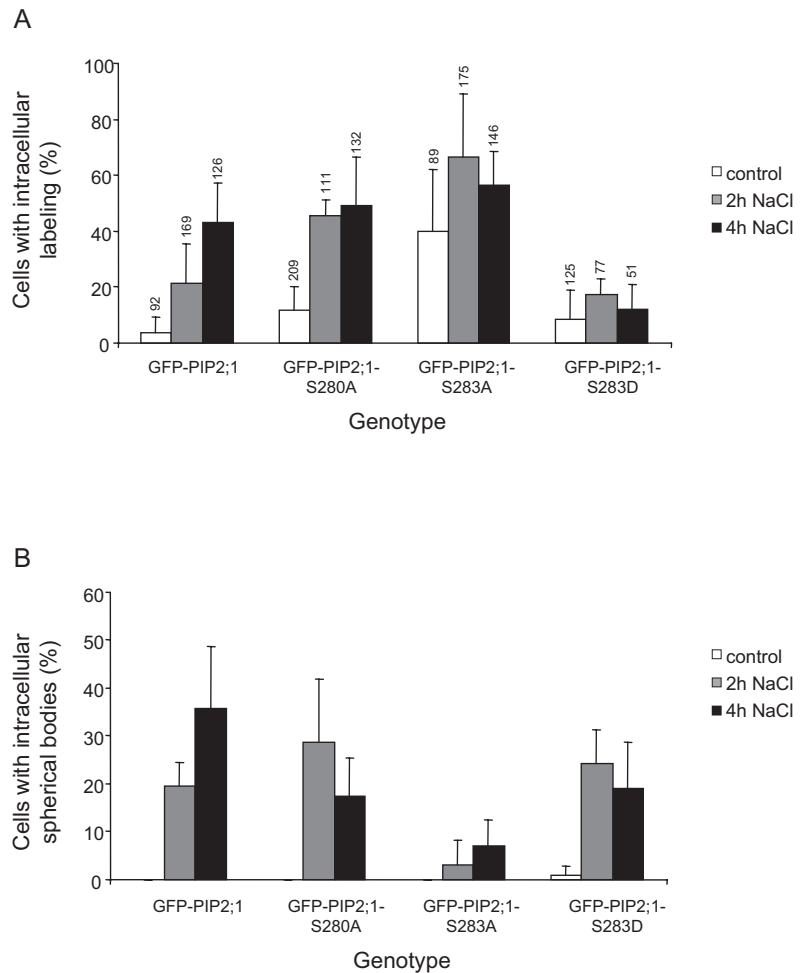


**FIG. 8. Role of C-terminal phosphorylation in the subcellular localization of AtPIP2;1 in response to salinity.** The figure shows typical laser-scanning confocal micrographs of the fluorescence emitted by transgenic root cells located at 1 cm from the apex and expressing GFP-PIP2;1 (*A* and *B*), GFP-PIP2;1-S280A (*C* and *D*), GFP-PIP2;1-S283A (*E* and *F*), or GFP-PIP2;1-S283D (*G* and *H*). Plants were treated during 2 h (*A*, *C*, *E*, and *G*) or 4 h (*B*, *D*, *F*, and *H*) with 100 mM NaCl prior to microscopic observations. Scale bar, 20  $\mu$ m.

To investigate the role of C-terminal phosphorylation of AtPIP2;1 in its salt-induced subcellular relocalization, we used the same set of transgenic plants as above. Microscopic observations of root epidermal cells were performed specifically at 1 cm from the apex (Fig. 8). Treatment with 100 mM NaCl during 2 or 4 h induced an intracellular diffuse staining (hereafter referred to as fuzzy staining) in up to 60% of root cells of plants expressing GFP-WT-PIP2;1, GFP-PIP2;1-S280A, and GFP-PIP2;1-Ser283A proteins (Figs. 8, *A–F*, and 9*A*). A similar staining, but much less abundant, was observed in salt-treated plants expressing PIP2;1-S283D (Figs. 8, *G* and *H*, and 9*A*). These observations suggested that the accumulation of AtPIP2;1 in fuzzy intracellular compartments observed in response to an NaCl treatment requires a non-phosphorylated form of Ser<sup>283</sup>.

A 100 mM NaCl treatment also induced the labeling of small intracellular spherical bodies in up to 35% of root

**FIG. 9. Quantification of intracellular fuzzy staining (A) and of spherical bodies (B) in root cells upon an NaCl treatment.** The figure represents the proportion of root epidermal cells 1 cm far from the apex that show intracellular fuzzy staining (A) and spherical bodies (B) in control conditions (*white*) and after treatment with 100 mM NaCl during 2 h (*gray*) or 4 h (*black*). Data were obtained from transgenic plants that express the following constructs: GFP-PIP2;1 (two independent transgenic lines;  $n \geq 7$  plants per treatment), GFP-PIP2;1-S280A (three independent transgenic lines;  $n = 9$  per treatment), GFP-PIP2;1-S283A (two independent transgenic lines;  $n \geq 7$  per treatment), and GFP-PIP2;1-S283D (two independent transgenic lines;  $n \geq 6$ , per treatment). The *numbers* on the graph correspond to the total number of observed cells and are identical in the two figures. The *error bars* represent S.D.



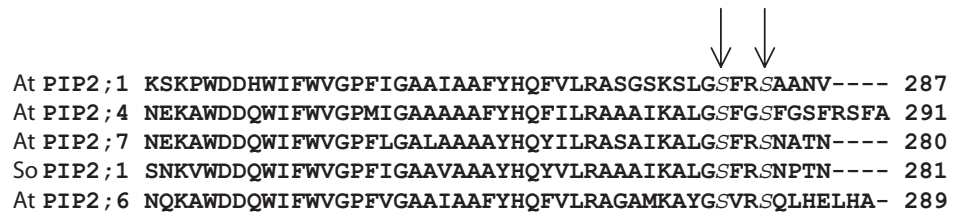
cells of plants expressing GFP-PIP2;1 (Figs. 8, A and B, and 9B). Although these bodies might be related to the endosome/prevacuolar compartment (40),<sup>2</sup> their precise nature remains uncertain. Salt-treated plants expressing GFP-PIP2;1-S280A and GFP-PIP2;1-S283D showed the same proportion of cells with these spherical structures (Figs. 8, C, D, G, and H, and 9B). By contrast, this type of labeling was almost not visible in root cells expressing GFP-PIP2;1-S283A (Figs. 8, E and F and 9B). These data suggested that residue Ser<sup>283</sup>, and very likely its phosphorylated form, is required during the salt-induced relocalization of AtPIP2;1 in intracellular spherical bodies.

#### DISCUSSION

The present work reports an original proteomics strategy to investigate the phosphorylation of AtPIP aquaporins in the *Arabidopsis* root. Three major steps were involved: (i) an enrichment in aquaporins from purified root PM, (ii) a subsequent enrichment in corresponding phosphopeptides by affinity purification on TiO<sub>2</sub> columns, and (iii) the identification of phosphoresidues by MALDI/TOF-TOF. The present work was focused on the C-terminal tail of AtPIPs, and

overall nine sites were identified in AtPIP2;1 (and/or AtPIP2;2 and AtPIP2;3), AtPIP2;4, and AtPIP2;7. In support for the enhanced resolution of our successive enrichment procedure, we note that six of these sites had not been described previously. AtPIP2;6 recently has been reported to be phosphorylated (25) but is not expressed in roots (12, 31). The present work also shows that bioinformatics predictions of phosphorylation sites cannot be substituted by an experimental identification of sites by MS. For instance, three Ser residues (Ser<sup>273</sup>, Ser<sup>277</sup>, and Ser<sup>280</sup>) were predicted using NetPhos software to be phosphorylated in the C-terminal tail of AtPIP2;1, whereas the experimental data established the phosphorylation of Ser<sup>280</sup> and that of an unpredicted site (Ser<sup>283</sup>). Similar discrepancies were observed for AtPIP2;4 and AtPIP2;7 (not shown). Our analysis also identified the phosphorylation of a Thr residue in PIP2;7, a modification that had never been formally described in aquaporins. A remarkable feature of AtPIPs is the presence of multiple, up to three, adjacent phosphorylations on their C-terminal tail. The amino acid sequence alignment of SoPIP2;1, AtPIP2;1, AtPIP2;4, AtPIP2;6, and AtPIP2;7 revealed a correspondence between the first two adjacent

FIG. 10. Sequence alignment of C-terminal phosphorylated plant aquaporins. Arrows indicate residues that can be phosphorylated and that are common between the isoforms.



phosphorylated Ser residues of these proteins (Fig. 10). Whereas independent phosphorylation at  $n$  sites yields in theory  $2^n$  peptide forms, we observed a reduced number of phosphorylated forms in *AtPIP2;1*, *AtPIP2;4*, and *AtPIP2;7*. In all three isoforms, phosphorylation of a site was apparently linked to phosphorylation of the closest site, upstream in the peptide sequence, or exceptionally to the second closest site in the case of Ser<sup>289</sup> of *AtPIP2;4*. Interdependent phosphorylation events could result from either a processive or a distributive functioning of the protein kinase along the C-terminal tail (41–43). In the case of *PIP2;1*, we observed that an S280A mutation did not alter the cellular expression of a GFP-*PIP2;1* fusion, whereas an S283A mutation did (Fig. 7). This suggests that phosphorylation of Ser<sup>283</sup> can occur in the GFP-*PIP2;1*-S280A form in the absence of phosphorylation at position 280. Therefore, we favor a distributivity mechanism whereby a similar protein kinase would act on the two sites with a greater efficiency on Ser<sup>280</sup>. Similar mechanisms may also be present in animal aquaporins because up to four phosphorylated serine residues have been identified in the C-terminal tail of mammalian aquaporin-2, and a putative interdependency was observed between phosphorylation of two of these sites (Ser<sup>256</sup> and Ser<sup>261</sup>) (44).

Although the present study represents a comprehensive analysis of C-terminal phosphorylation of *AtPIP2* aquaporins expressed in roots, other aquaporin phosphorylation sites surely remain to be uncovered. *AtPIP1* isoforms represent in addition to *AtPIP2* abundant proteins in the 28-kDa SDS-PAGE band (31, 33). Although the C-terminal tail of *AtPIP1* is not predicted to be phosphorylated, we attempted to detect phosphopeptides derived from this domain. However, the digestion of *AtPIP1* isoforms with several different proteolytic enzymes that should release C-terminal *AtPIP1* did not allow detection of these domains (data not shown). A phosphorylation site conserved in loop *B* of all plant PIP isoforms has been postulated based on immunodetection with an anti-phosphopeptide antibody (45) or functional characterization of site-directed mutants in *Xenopus* oocytes (22). Here again, the corresponding native or phosphorylated peptide could not be detected by MS possibly because of low efficiency of the enzyme digestion, the confinement of these peptides into acrylamide after digestion, or also a low ionization efficiency of these peptides. With recent developments in Fourier transform mass spectrometry and the introduction of dissociation modes other than CID, top-down proteomics may be useful to uncover additional phosphorylation sites (46, 47).

An absolute quantification procedure was developed to quantify the relative abundance of the unmodified, singly, and diphosphorylated forms of *AtPIP2;1*. Plants growing in normal conditions showed a 1:1:2 relative abundance ratio, indicating that *AtPIP2;1* is mainly diphosphorylated in the root PM. We also investigated the effects on *AtPIP2;1* phosphorylation of NaCl and H<sub>2</sub>O<sub>2</sub> treatments, two stimuli known to typically induce a rapid inhibition of *L<sub>p,r</sub>* in *Arabidopsis* (12).<sup>2</sup> In these experiments it was of importance to systematically sequence all singly and diphosphorylated forms of *AtPIP2;1*. Because no phosphorylation of Ser<sup>277</sup> was observed in any of the treatments, our quantitative data can truly be interpreted as reversible changes of phosphorylation at Ser<sup>280</sup> and Ser<sup>283</sup>. NaCl induced a 30% decrease in the level of Ser<sup>283</sup> phosphorylation together with a tendency for an increased relative abundance of the singly and unphosphorylated forms (Fig. 6A). By contrast, an H<sub>2</sub>O<sub>2</sub> treatment increased by 20% the relative abundance of the diphosphorylated form and decreased the abundance of the unmodified form (Fig. 6B). Thus, the *AtPIP2;1* phosphorylation status appears to be highly sensitive to environmental stimuli acting on root water transport. However, the changes in *AtPIP2;1* phosphorylation were not unequivocally associated to changes in *L<sub>p,r</sub>*. Because they were of modest amplitude, neither one of these changes may be sufficient to account for the strong decrease in *L<sub>p,r</sub>* induced by the two stimuli. Thus, additional mechanisms including altered phosphorylation of other root aquaporins (*AtPIP2;4*, *AtPIP2;7*, or others) or other as yet unidentified regulatory mechanisms may contribute to the decrease in *L<sub>p,r</sub>*. Phosphorylation at Ser<sup>274</sup> of *SoPIP2;1*, the spinach homologue of *AtPIP2;7*, was shown to be decreased in leaves under reduced water potential (hyperosmotic treatment) (22). By contrast, phosphorylation of the corresponding residue in *AtPIP2;1* (Ser<sup>280</sup>) was insensitive to NaCl treatment, whereas phosphorylation of Ser<sup>283</sup> was decreased. In nitrogen-fixing nodules of soybean roots, phosphorylation of the aquaporin Nodulin-26 on a C-terminal serine residue (Ser<sup>262</sup>) was enhanced upon a water stress (21). These different observations may be explained by differences in the aquaporin isoform and the tissue considered. Recent results on mammalian aquaporin-2 have also revealed reciprocal changes in phosphorylation of two C-terminal serine residues (Ser<sup>256</sup> and Ser<sup>261</sup>) in response to vasopressin exposure, suggesting that these residues may serve distinct roles in aquaporin-2 regulation (44, 48). Overall these different studies point to a critical role for aquaporin phosphorylation in response to various physiological contexts and emphasize the need for a global view of aquaporin

phosphorylation dynamics. In these respects, the present study justifies the development of novel, more comprehensive MS-based strategies based on multiple reaction monitoring and/or stable isotope labeling (14).

Functional and structural analyses in spinach SoPIP2;1 have indicated a role for Ser<sup>274</sup> in gating the aquaporin (8, 22). By contrast, a possible role for this or the equivalent site in AtPIP2;1 (Ser<sup>280</sup>) in controlling aquaporin trafficking has remained unexplored. In addition, the functional significance of the adjacent phosphorylation site (Ser<sup>283</sup> in AtPIP2;1) has remained totally unknown. Here we found that this phosphosite was specifically involved in the response of *Arabidopsis* roots to NaCl. Therefore, we focused on the role of the two sites (Ser<sup>280</sup> and Ser<sup>283</sup>) in AtPIP2;1 trafficking under normal or NaCl stress conditions. For this, we expressed in transgenic *Arabidopsis* GFP-PIP2;1 fusions carrying Ser to Ala mutations to abolish phosphorylation or Ser to Asp mutations to possibly mimic a constitutive phosphorylation. A S280A mutation did not affect the localization profile of the fusion protein when compared with that of wild type GFP-PIP2;1 (Fig. 7). By contrast, an S283A but not an S283D mutation prevented a proper transfer of the protein at the PM (Fig. 7). These results allow us to exclude a detrimental effect of Ser<sup>283</sup> removal and rather indicate that phosphorylation of this residue, but not of Ser<sup>280</sup>, is necessary for the subcellular trafficking of AtPIP2;1. The perinuclear staining displayed by GFP-PIP2;1-S283A suggests an accumulation in the ER. Therefore, phosphorylation of AtPIP2;1 at Ser<sup>283</sup> seems to favor export of the protein from the ER. A similar model was proposed for mammalian aquaporin-2 whereby phosphorylation of Ser<sup>256</sup> by two distinct protein kinases, with different subcellular localizations, mediates the exit of the aquaporin from the Golgi complex and subsequently its translocation from vesicular compartments to the PM (28).

One of the marked effects of an NaCl treatment was to exacerbate the staining by PIP2;1-GFP of diffuse intracellular structures. These intracellular structures were similar to those stained by GFP-PIP2;1-S283A in resting conditions. Mutant analysis showed in addition that the NaCl effects were less pronounced specifically in GFP-PIP2;1-S283D and therefore may be counteracted by phosphorylation of Ser<sup>283</sup> (Fig. 9A). These results suggest that NaCl acts on AtPIP2;1 with unphosphorylated Ser<sup>283</sup> to favor its intracellular accumulation. However, we cannot distinguish at present between (i) an intracellular retention or a misrouting of neosynthesized proteins on their route to the PM and (ii) a relocalization of proteins from the PM into intracellular compartments. NaCl also induced the labeling of intracellular spherical bodies in transgenic plants expressing GFP-PIP2;1. The precise nature of these structures remains to be elucidated, but due to their size (1–5  $\mu\text{m}$ ) and spherical form, they may be related to the prevacuolar/multivesicular body compartment<sup>2</sup> and devoted to protein degradation. GFP-PIP2;1-S280A and GFP-PIP2;1-S283D, but not GFP-PIP2;1-S283A, labeled the

spherical bodies in NaCl-treated roots (Fig. 9B) suggesting that phosphorylation at position 283 was required for relocalization of AtPIP2;1 in this compartment. In summary, an NaCl treatment induced an intracellular accumulation of AtPIP2;1 by exerting specific actions onto AtPIP2;1 forms differing in their phosphorylation at Ser<sup>283</sup> to induce their accumulation in distinct intracellular structures. It is noteworthy that NaCl also induced dephosphorylation of Ser<sup>283</sup> as was observed on a purified PM fraction. This may reflect a compensatory mechanism to prevent the relocalization of the phosphorylated AtPIP2;1 in spherical bodies and thus to slow down its degradation. Therefore, a fine and reversible tuning of aquaporin density at the cell surface may be achieved.

In conclusion, aquaporin phosphorylation appears to be a significant target in plants under stress. The present study documents salt-induced quantitative changes in aquaporin phosphorylation and establishes, for the first time, a link with aquaporin subcellular localization. Similar links will have to be investigated in contexts such as stress or nutrient responses where information on aquaporin phosphorylation or trafficking has recently emerged (25).<sup>2</sup>

*Acknowledgments*—We thank Sabrina Laugesen, Thibaud Adam, and Valérie Rofidal for help and technical advice in proteomics. Confocal microscopy observations were made at the Montpellier Réunion Inter-Organismes Imaging facility with the financial support of the Federative Research Institute (Daphne) “Développement, Diversité et Adaptation des Plantes.”

\* This work was supported by INRA Grant AgroBI AIP300. The costs of publication of this article were defrayed in part by the payment of page charges. This article must therefore be hereby marked “advertisement” in accordance with 18 U.S.C. Section 1734 solely to indicate this fact.

§ The on-line version of this article (available at <http://www.mcponline.org/>) contains supplemental material.

¶ Present address: plate-forme de protéomique, Institut Pasteur, 28 rue du Docteur Roux, F-75724 Paris cedex 15, France.

|| To whom correspondence should be addressed. Tel.: 33-4-99-61-20-20; Fax: 33-4-67-52-57-37; E-mail: [santoniv@supagro.inra.fr](mailto:santoniv@supagro.inra.fr).

## REFERENCES

1. Kaldenhoff, R., and Fischer, M. (2006) Functional aquaporin diversity in plants. *Biochim. Biophys. Acta* **1758**, 1134–1141
2. Maurel, C. (2007) Plant aquaporins: novel functions and regulation properties. *FEBS Lett.* **581**, 2227–2236
3. Vandeleur, R., Niemietz, C. M., Tilbrook, J., and Tyerman, S. D. (2005) Role of aquaporins in root responses to irrigation. *Plant Soil* **274**, 141–161
4. Johanson, U., Karlsson, M., Johansson, I., Gustavsson, S., Sjövall, S., Frayssé, L., Weig, A. R., and Kjellbom, P. (2001) The complete set of genes encoding major intrinsic proteins in *Arabidopsis* provides a framework for a new nomenclature for major intrinsic proteins in plants. *Plant Physiol.* **126**, 1–12
5. Quigley, F., Rosenberg, J. M., Shachar-Hill, Y., and Bohnert, H. J. (2002) From genome to function: the *Arabidopsis* aquaporins. *Genome Biol.* **3**, 1–17
6. Zardoya, R., and Villalba, S. (2001) A phylogenetic framework for the aquaporin family in eukaryotes. *J. Mol. Evol.* **52**, 391–404
7. Fujiyoshi, Y., Mitsuoka, K., de Groot, B. L., Philippsen, A., Grubmüller, H., Agre, P., and Engel, A. (2002) Structure and function of water channels. *Curr. Opin. Struct. Biol.* **12**, 509–515

8. Tornroth-Horsefield, S., Wang, Y., Hedfalk, K., Johanson, U., Karlsson, M., Tajkhorshid, E., Neutze, R., and Kjellbom, P. (2006) Structural mechanism of plant aquaporin gating. *Nature* **439**, 688–694
9. Chaumont, F., Moshelion, M., and Daniels, M. J. (2005) Regulation of plant aquaporin activity. *Biol. Cell* **97**, 749–764
10. Luu, D.-T., and Maurel, C. (2005) Aquaporins in a challenging environment: molecular gears for adjusting plant water status. *Plant Cell Environ.* **28**, 85–96
11. Javot, H., and Maurel, C. (2002) The role of aquaporins in root water uptake. *Ann. Bot.* **90**, 301–313
12. Boursiac, Y., Chen, S., Luu, D.-T., Sorieul, M., van den Dries, N., and Maurel, C. (2005) Early effects of salinity on water transport in *Arabidopsis* roots. Molecular and cellular features of aquaporin expression. *Plant Physiol.* **139**, 790–805
13. Lee, S. H., Singh, A. P., and Chung, G. C. (2004) Rapid accumulation of hydrogen peroxide in cucumber roots due to exposure to low temperature appears to mediate decreases in water transport. *J. Exp. Bot.* **55**, 1733–1741
14. Wolf-Yadlin, A., Hautaniemi, S., Lauffenburger, D. A., and White, F. M. (2007) Multiple reaction monitoring for robust quantitative proteomic analysis of cellular signaling networks. *Proc. Natl. Acad. Sci. U. S. A.* **104**, 5860–5865
15. Jensen, O. N. (2004) Modification-specific proteomics: characterization of post-translational modifications by mass spectrometry. *Curr. Opin. Chem. Biol.* **8**, 33–41
16. Bennett, K. L., Stensballe, A., Podtelejnikov, A. V., Moniatte, M., and Jensen, O. N. (2002) Phosphopeptide detection and sequencing by matrix-assisted laser desorption/ionization quadrupole time-of-flight tandem mass spectrometry. *J. Mass Spectrom.* **37**, 179–190
17. Stensballe, A., and Jensen, O. N. (2004) Phosphoric acid enhances the performance of Fe(III) affinity chromatography and matrix-assisted laser desorption/ionization tandem mass spectrometry for recovery, detection and sequencing of phosphopeptides. *Rapid Commun. Mass Spectrom.* **18**, 1721–1730
18. Zhou, W., Merrick, B. A., Khaledi, M. G., and Tomer, K. B. (2000) Detection and sequencing of phosphopeptides affinity bound to immobilized metal ion beads by matrix-assisted laser desorption/ionization mass spectrometry. *J. Am. Soc. Mass Spectrom.* **11**, 273–282
19. Larsen, M. R., Thingholm, T. E., Jensen, O. N., Roepstorff, P., and Jorgensen, T. J. (2005) Highly selective enrichment of phosphorylated peptides from peptide mixtures using titanium dioxide microcolumns. *Mol. Cell. Proteomics* **4**, 873–886
20. Daniel, J. A., and Yeager, M. (2005) Phosphorylation of aquaporin PvTIP3;1 defined by mass spectrometry and molecular modeling. *Biochemistry* **44**, 14443–14454
21. Guenther, J. F., Chanmanivone, N., Galetovic, M. P., Wallace, I. S., Cobb, J. A., and Roberts, D. M. (2003) Phosphorylation of soybean nodulin 26 on serine 262 enhances water permeability and is regulated developmentally and by osmotic signals. *Plant Cell* **15**, 981–991
22. Johansson, I., Karlsson, M., Shukla, V. K., Chrispeels, M. J., Larsson, C., and Kjellbom, P. (1998) Water transport activity of the plasma membrane aquaporin PM28A is regulated by phosphorylation. *Plant Cell* **10**, 451–459
23. Johansson, I., Larsson, C., Ek, B., and Kjellbom, P. (1996) The major integral proteins of spinach leaf plasma membranes are putative aquaporins and are phosphorylated in response to  $Ca^{2+}$  and apoplastic water potential. *Plant Cell* **8**, 1181–1191
24. Miao, G.-H., Hong, Z., and Verma, D. P. S. (1992) Topology and phosphorylation of soybean nodulin-26, an intrinsic protein of the peribacteroid membrane. *J. Cell Biol.* **118**, 481–490
25. Niittylä, T., Fuglsang, A. T., Palmgren, M. G., Frommer, W. B., and Schulze, W. X. (2007) Temporal analysis of sucrose-induced phosphorylation changes in plasma membrane proteins of *Arabidopsis*. *Mol. Cell. Proteomics* **6**, 1711–1726
26. Nühse, T. S., Stensballe, A., Jensen, O. N., and Peck, S. C. (2004) Phosphoproteomics of the *Arabidopsis* plasma membrane and a new phosphorylation site database. *Plant Cell* **16**, 2394–2405
27. Kamsteeg, E.-J., Heijnen, I., van Os, C. H., and Deen, P. M. T. (2000) The subcellular localization of an aquaporin-2 tetramer depends on the stoichiometry of phosphorylated and non phosphorylated monomers. *J. Cell Biol.* **151**, 919–929
28. Procino, G., Carmosino, M., Marin, O., Brunanti, A. M., Contri, A., Pinna, L., Mannucci, R., Nielsen, S., Kwon, T.-H., Svelto, M., and Valenti, G. (2003) Ser-256 phosphorylation dynamics of aquaporin 2 during maturation from the endoplasmic reticulum to the vesicular compartment in renal cells. *FASEB J.* **17**, 1886–1910
29. Barkla, B. J., Vera-Estrella, R., Pantoja, O., Kirch, H.-H., and Bohnert, H. J. (1999) Aquaporin localization—how valid are the TIP and PIP labels. *Trends Plant Sci.* **4**, 86–88
30. Kirch, H. H., Vera-Estrella, R., Gollack, D., Quigley, F., Michalowski, C. B., Barkla, B. J., and Bohnert, H. J. (2000) Expression of water channel proteins in *Mesembryanthemum crystallinum*. *Plant Physiol.* **123**, 111–124
31. Santoni, V., Vinh, J., Pflieger, D., Sommerer, N., and Maurel, C. (2003) A proteomic study reveals novel insights into the diversity of aquaporin forms expressed in the plasma membrane of plant roots. *Biochem. J.* **373**, 289–296
32. Murashige, T., and Skoog, F. (1962) A revised medium for rapid growth and bioassays with tobacco tissue cultures. *Physiol. Plant.* **15**, 473–497
33. Santoni, V., Verdoucq, L., Sommerer, N., Vinh, J., Pflieger, D., and Maurel, C. (2006) Methylation of aquaporins in plant plasma membrane. *Biochem. J.* **400**, 189–197
34. Hem, S., Rofidal, V., Sommerer, N., and Rossignol, M. (2007) Novel subsets of the *Arabidopsis* plasmalemma phosphoproteome identify phosphorylation sites in secondary active transporters. *Biochem. Biophys. Res. Commun.* **363**, 375–380
35. Hellens, R. P., Edwards, E. A., Leyland, N. R., Bean, S., and Mullineaux, P. M. (2000) pGreen: a versatile and flexible binary Ti vector for *Agrobacterium*-mediated plant transformation. *Plant Mol. Biol.* **42**, 819–832
36. Clough, S. J., and Bent, A. F. (1998) Floral dip: a simplified method for *Agrobacterium*-mediated transformation of *Arabidopsis thaliana*. *Plant J.* **16**, 735–743
37. Alexandersson, E., Fraysse, L., Sjøvall-Larsen, S., Gustavsson, S., Fellert, M., Karlsson, M., Johanson, U., and Kjellbom, P. (2005) Whole gene family expression and drought stress regulation of aquaporins. *Plant Mol. Biol.* **59**, 469–484
38. Gerber, S. A., Rush, J., Stemman, O., Kirschner, M. W., and Gygi, S. (2003) Absolute quantification of proteins and phosphoproteins from cell lysates by tandem MS. *Proc. Natl. Acad. Sci. U. S. A.* **100**, 6940–6945
39. Hawes, C., Saint-Jore, C. M., Brandizzi, F., Zheng, H., Andreeva, A. V., and Boevink, P. (2001) Cytoplasmic illuminations: in planta targeting of fluorescent proteins to cellular organelles. *Protoplasma* **215**, 77–88
40. Müller, J., Mettlich, U., Menzel, D., and Samaj, J. (2007) Molecular dissection of endosomal compartments in plants. *Plant Physiol.* **145**, 293–304
41. Aubol, B. E., Chakrabarti, S., Ngo, J., Shaffer, J., Nolen, B., Fu, X. D., Ghosh, G., and Adams, J. A. (2003) Processive phosphorylation of alternative splicing factor/splicing factor 2. *Proc. Natl. Acad. Sci. U. S. A.* **100**, 12601–12606
42. Gunawardena, J. (2005) Multisite protein phosphorylation makes a good threshold but can be a poor switch. *Proc. Natl. Acad. Sci. U. S. A.* **102**, 14617–14622
43. Waas, W. F., Lo, H. H., and Dalby, K. N. (2001) The kinetic mechanism of the dual phosphorylation of the ATF2 transcription factor by p38 mitogen-activated protein (MAP) kinase  $\alpha$ . Implications for signal/response profiles of MAP kinase pathways. *J. Biol. Chem.* **276**, 5676–5684
44. Hoffert, J. D., Pisitkun, T., Wang, G., Shen, R. F., and Knepper, M. A. (2006) Quantitative phosphoproteomics of vasopressin-sensitive renal cells: regulation of aquaporin-2 phosphorylation at two sites. *Proc. Natl. Acad. Sci. U. S. A.* **103**, 7159–7164
45. Aroca, R., Amodeo, G., Fernandez-Illescas, S., Herman, E. M., Chaumont, F., and Chrispeels, M. J. (2005) The role of aquaporins and membrane damage in chilling and hydrogen peroxide induced changes in the hydraulic conductance of maize roots. *Plant Physiol.* **137**, 341–353
46. Bogdanov, B., and Smith, R. D. (2005) Proteomics by FTICR mass spectrometry: top down and bottom up. *Mass Spectrom. Rev.* **24**, 168–200
47. Gómez, S. M., Nishio, J. N., Faull, K. F., and Whitelegge, J. P. (2002) The chloroplast grana proteome defined by intact mass measurements from liquid chromatography mass spectrometry. *Mol. Cell. Proteomics* **1**, 46–59
48. Hoffert, J. D., Nielsen, J., Yu, M. J., Pisitkun, T., Schleicher, S. M., Nielsen, S., and Knepper, M. A. (2007) Dynamics of aquaporin-2 serine-261 phosphorylation in response to short-term vasopressin treatment in collecting duct. *Am. J. Physiol.* **292**, F691–F700